EMPIRICAL MAPPING OF THE CONVECTIVE HEAT TRANSFER COEFFICIENTS WITH LOCAL HOT SPOTS ON HIGHLY CONDUCTIVE SURFACES

by
Murat TEKELİOĞLU
Department of Mechanical Engineering, Karabük University,
Karabük 78050, TURKEY

An experimental method was proposed to assess the natural and forced convective heat transfer coefficients on highly conductive bodies. Experiments were performed at air velocities of $0m/s$, $4.0m/s$, *and* $5.4m/s$, *and comparisons were made between the current results and available literature. These experiments were extended to arbitrary-shape bodies. External flow conditions were maintained throughout. In the proposed method, in determination of the surface convective heat transfer coefficients, flow condition is immaterial, i.e., either laminar or turbulent. With the present method, it was aimed to acquire the local heat transfer coefficients on any arbitrary conductive shape. This method was intended to be implemented by the heat transfer engineer to identify the local heat transfer rates with local hot spots. Finally, after analyzing the proposed experimental results, appropriate decisions can be made to control the amount of the convective heat transfer off the surface. Limited mass transport was quantified on the cooled plate.*

Key words: *Arbitrary shape, conductive body, local spot, natural convection, forced convection*

1. Literature

Convective heat transfer has been the subject of many research. A brief summary of these studies is included here: Mixed convection condition was theoretically analyzed on the vertical plate fin to demonstrate the effect of the conjugate convection-conduction parameter on the fin temperature distribution, local heat transfer coefficient, local heat flux, overall heat transfer rate, and fin efficiency [1]. It was shown that the near-wall porosity variation increased the rate of the heat transfer. A conductive fin was exploited numerically with different Ri numbers [2]. Conjugate mixed convection was considered with governing equations on the other flat-plate fin geometry [3]. Under opposing and assisting mixed convection, mixed convection heat transfer coefficients were given on the vertical flat plate under constant heat flux condition [4]. Natural convection heat transfer coefficients were theoretically derived and next numerically solved for the horizontal, inclined, and vertical flat plates in which the wall temperature (T_w) and surface heat flux (q_w) varied with the axial coordinate x [5]. There, the authors found that the local wall shear stress and the local surface heat transfer rate both increased with the inclination angle and Grashof number. Natural convection was theoretically studied on the infinitely long vertical channels and finite vertical channels and pipes through localized heat generation on the centerline and isothermal walls elsewhere [6]. In their work, optimum channel height and Rayleigh number limit issues were discussed. Heating and cooling effect on the buoyancy flow was theoretically studied on the

two-dimensional stretched oblique vertical plate [7]. Authors stated there that the mixed convection parameter affected the location of the zero skin-friction (zero shear stress) on the isothermal plate. In another modeling, a heat convection length (Δs) was introduced to replace the convective heat transfer coefficient average ($\bar{h}$) given in the literature for a) the forced convection over the horizontal plate and b) the free convection over the vertical plate [8]. In that work, it was aimed to give a representative $\bar{h}$ for the cases. $Prandtl$ number range given previously of the natural convection over the arbitrary-shape three-dimensional bodies was extended to cover a wider range $0.71 \lesssim Pr \lesssim 2{,}000$ [9]. Although $Pr = 0.71$ was included, the authors compared their equations extensively with the experimental results of the other researchers for $5.8 < Pr < 14$, $Pr = 6.0$, $Pr = 1{,}800$, and $Pr = 2{,}000$. Convection heat transfer regimes; natural convection, laminar forced convection, or mixed convection, were numerically studied on the heated moving vertical plate with uniform and non-uniform suction/injection at the surface [10]. Free convection problem was theoretically studied and later numerically solved on the axisymmetric and two-dimensional bodies of the arbitrary shape in a porous medium [11]. It was noted that the heat convection depended on the yield stress of the boundary. The two-dimensional natural convection problem was solved numerically on the vertical convergent channel having a convergence angle of θ [12]. Local $Nusselt$ number and temperature distributions were given. External natural convection was theoretically studied on the two-dimensional bodies in a saturated porous medium under constant heat flux [13]. A diffusivity characteristic body length ($\sqrt{A}$) was introduced on Reynolds and Nusselt numbers as the square root of the total surface area (A) with the characteristic body length ($\mathcal{L}$) to semi-empirically study the laminar forced convection from spheroids [14]. Laminar natural convection heat transfer from the arbitrary geometries into the extensive stagnant fluid was modeled [15]. Turbulent free convection heat transfer from the arbitrary geometries to non-Newtonian power-law fluids was studied using the Nakayama-Koyama solution [16]. Their surface wall temperature was allowed to vary in an arbitrary fashion. Conjugated effect of the heat conduction and natural convection was modeled inside and around the arbitrary shape and solved with the NAPPLE algorithm and SIS solver [17].

It was observed from the outlined literature that when the materials (fins, for example) used in the heat transfer process were metallic, a theoretical solution (numerical or analytical) was given. It was pointed out by the current author that when the heat transfer surface was of a metallic material of high thermal diffusivity such as aluminum then experimental results correspondingly became unrealistic. That is to say, when the heat transfer boundaries are created with a highly conductive material, the experimental heat transfer analysis is more complex than a theoretical heat transfer analysis. It is concluded in this paper that the experimental natural and forced convective heat transfer coefficient values of a highly conductive medium are unrealistic. In the present study, an experimental local hot spot approach is presented on the highly conductive heat transfer surfaces. These experiments were extended to the arbitrary-shape bodies.

2. Theme

In the forced convection, $Nu = f(Re, Pr)$ where Nu is the $Nusselt$ number ($Nu = (hx)/k$) based on the characteristic length x, Re is the $Reynolds$ number ($Re = (u_\infty x)/\nu$) of the flow, and Pr is the $Prandtl$ number of the fluid ($Pr = \nu/\alpha$). Maintaining external flow conditions, if the surface over which a specific type of fluid flows is highly conductive, only theoretical expressions give realistic information on such geometries as horizontal flat plate or vertical flat plate with natural convection or forced convection present. Investigating these geometries experimentally when the material is highly conductive is equally important,

because it sets the basis for comparisons between the available theoretical expressions. In this paper, initially, the experimental results were compared with the expressions given in the literature extensively: free convection of the heated horizontal flat plate, forced convection of the heated horizontal flat plate, and free convection of the heated vertical flat plate. Then, the experimental results were presented on the arbitrary-shape bodies. The present experimental apparatus simulated the highly conductive surface and was an experimentally discretized surface.

The quantity assessment of the convective heat transfer from the arbitrary-shape bodies is important as it is hard to obtain the convective heat transfer coefficients on the arbitrary-shape bodies maintaining external flow conditions. This is because of the fact that for the arbitrary-shape bodies, it is a little bit of a complicated task to establish and acquire Nu accurately. The reasons for this are those: 1) Velocity and thermal boundary layer developments are different from those identified on the flat plates. For example, the flow separation may take place on the arbitrary-shape bodies. 2) Turbulent flow condition may be present accompanied by the vortices on the arbitrary-shape body. These conditions can be investigated theoretically, i.e., either numerically or analytically. It is yet another alternative to investigate the convective heat transfer coefficients on the arbitrary-shape bodies experimentally. An experimental approach of this nature becomes informative, besides the theoretical studies, to map out the local natural and local forced convective heat transfer coefficients. With the acquired experimental convective heat transfer coefficients, focus can be shifted toward the spots on which the natural or forced convective heat transfer rates can be calculated.

3. Highly Conductive Surface

In order to prepare the experimental setup, a substrate made of a play-dough type material was purchased and twelve plates ($2cmx2cmx1mm$) made of aluminum ($\mathrm{EN-AW\ 1050},\ 99.5\%\ Al$, [18]) were cut out. Surface condition of each plate was visually free from any major defects, therefore, each aluminum plate was accepted as identical and smooth surface. Electrical resistors with resistivity values of $1\Omega \pm 5\%$ were attached (adhered) to the plates (Fig. 1). The substrate dough material was decorated with plates each holding a resistor. Hence, a total number of twelve plates with twelve resistors were placed on the substrate material creating the highly conductive surface. The created highly conductive surface was a discretized surface. A total number of twelve plates was chosen here but this number can be made smaller or larger depending on the surface.

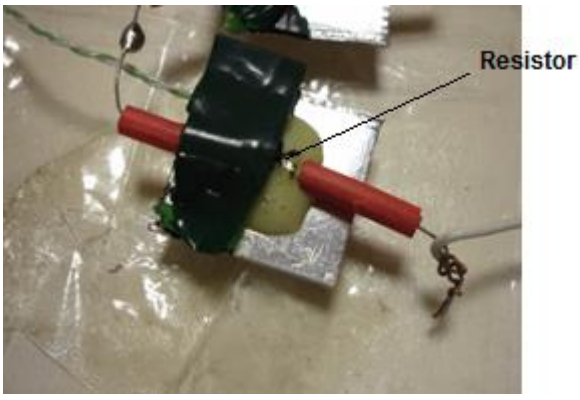

Fig. 1. A resistor shown attached (adhered) to the aluminum plate.

4. Instrumentation

An air fan with two levels of speed control was used in the experiments. Air velocities of $u_\infty = 4.0\text{m/s}$ and $u_\infty = 5.4\text{m/s}$ were measured with an anemometer (Model: DT-618, [19]) at the entrance of the first plate. The local natural and local forced convective heat transfer coefficients were assessed with the local hot spots created on the plates. A Type K thermocouple (PTFE insulated, exposed wire, [20]) was attached to each plate with the help of an adhesive tape. Fig. 2 shows the horizontal flat plate created with twelve plates.

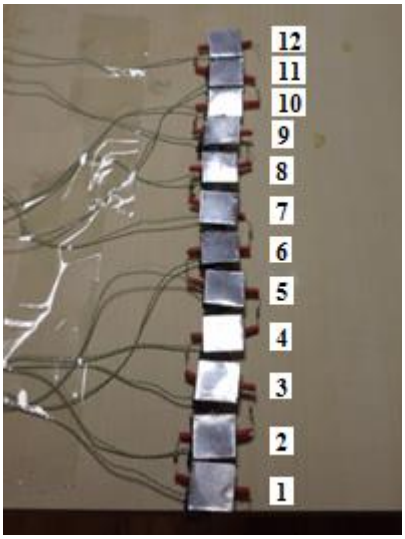

Fig. 2. Horizontal flat plate created with twelve plates. Plate numbers identified on each plate.

Single temperature readings were taken from each plate. The two data loggers of the same type, each with an eight-channel capacity, were attached to the personal computer. Plate temperatures were simultaneously recorded by the data acquisition device (Type USB TC-08 Thermocouple Data logger, [21]). Fig. 3 illustrates the experimental setup.

Fig. 3. Experimental setup in the assessment of the experimental convective heat transfer coefficients on the conductive surfaces. Centered is the arbitrary-shape body.

It was observed from the preliminary results of the plate temperature measurements that irregular resistor and thermocouple placements on the plates were creating temperature non-uniformities on the measured values. To suppress this negative effect, the readings of the data loggers were calibrated with reference to the twelve-plate average temperature of $54.457℃$ (with a standard deviation, $\sigma = 2.7416℃$) of the horizontal flat plate with natural convection ($u_\infty = 0\mathrm{m/s}$). Fig. 4 shows the calibration of the horizontal flat plate temperature measurements. Temperature measurements were calibrated in reference to a horizontal flat plate ($u_\infty = 0\mathrm{m/s}$) and twelve-plate average temperature in fig. 4.

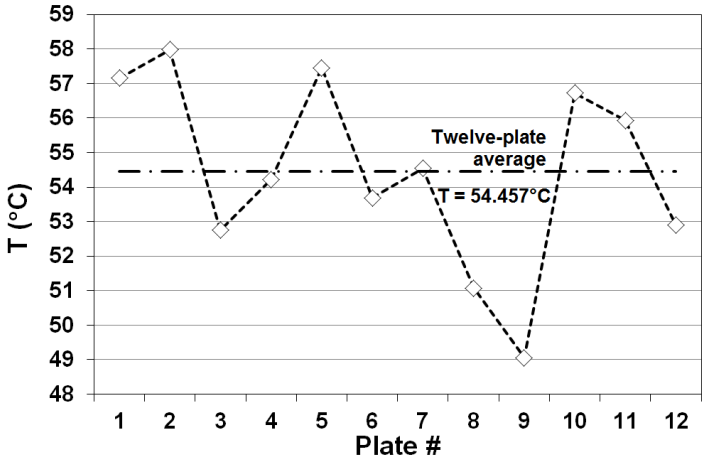

Fig. 4. Temperature measurements on the twelve plates. Irregular thermocouple and resistor placement affected the measurement results of these highly conductive surfaces. The temperature oscillations were viewed as experimental artifacts.

Fig. 4 was used to suppress the irregular thermocouple and resistor positioning effects. In the acquisition of the data, real-time continuous sampling was used: At about every $16\mathrm{ms}$, one temperature reading was taken until $100\mathrm{s}$ was reached after which acquisition was stopped. A proposed increase of the electrical resistance value, for example from 1Ω to 2.2Ω, was to decrease the power generation on the plates, thereby, to decrease the plate temperatures. Fig. 4 indicated in this paper that an experimental solution was not possible on highly-conductivity surfaces. The experiment on fig. 4 was repeated several times with the re-attachments of thermocouples and resistors to different aluminum plates. The results were, however, of non-uniform form as was shown here.

5. Results

The thermal conductivity value of the aluminum plates (k_{Al}) was measured across ($2cmx2cmx1mm$) plates. A value of $k_{Al} = 189.2\ \mathrm{W/(mK)}$ was calculated from the relation $k_{Al} = (q \cdot \Delta t)/(A_l \cdot (T_{s,1} - T_{s,2}))$ where $T_{s,1}$ and $T_{s,2}$ are, respectively, the local surface temperatures on the high temperature and low temperature sides ($T_{s,1} = 49.77℃$ and $T_{s,2} = 49.08℃$), $I = 0.59\mathrm{A}$ (a measured value), $R = 1\Omega$, $q = I^2R = (0.59\mathrm{A})^2 1\Omega \left(\frac{1}{2}\right) = 0.174\mathrm{W}$ (Assuming that $1/2$ of the total heat generation makes it way to the plate and the other half gets lost to the adhesive and the surroundings), $\Delta t = 10^{-3}\mathrm{m}$, and $A_l = 0.0133 \cdot 10^{-4}\mathrm{m}^2$ (resistor's estimated contact surface area). The value $k_{Al} = 189.2\ \mathrm{W/(mK)}$ calculated was lower than the value $k_{Al} = 237.0\ \mathrm{W/(mK)}$ listed for pure aluminum in the literature. As it can be deduced from the Bi definition, $Bi = (h_{avg}\Delta t)/k_{Al}$, when $Bi < 0.1$ each plate can be taken as having a uniform temperature throughout with h_{avg}

defined as the average convective heat transfer coefficient on the surface. Due to the high value of k_{Al}, a thin plate ($\Delta t = 10^{-3}m$), and a low value of h_{avg} ($h_{avg} = 19.776\mathrm{W/(m^2K)}$), $T_{s,2}$ can be taken as $T_{s,2} \cong T_{s,1}$. The heat equation, or $\alpha\left(\frac{d^2T}{dx^2}\right) = 0$, yields a free-surface temperature of 49.31℃ for a measured surface temperature of 50.0℃ on the thermocouple side. BCs are the conjugate convective and radiative heat transfer from each aluminum plate surface. In fact, heat was transferred from the both surfaces of the aluminum plates. Yet, the convection (forced or natural) was effective from the open surfaces of the aluminum plates.

5.1. Horizontal flat plate: forced convection

In the case of the constant heat flux ($q = const$), $Nu_x = 0.453(Re_x)^{1/2}(Pr)^{1/3}$ is given for the laminar flow ($Pr \gtrsim 0.6$) [22]. Average convective heat transfer coefficients of the plates were calculated with Nu_x from $h_{avg} = (1/L_p)\int_{x_1}^{x_2}\frac{k_{air}}{x}Nu_x dx$ where k_{air} is the temperature-dependent thermal conductivity of air ($\mathrm{W/(mK)}$), x_1 is the starting point $x-$coordinate of a plate along the flow direction (m), x_2 is the end point $x-$coordinate of a plate along the flow direction (m), and L_p is the length of the plate ($L_p = 2\mathrm{cm}$). In addition to this convective heat transfer, there will also be a surface radiation from the plates into the surroundings. Plate surface emissivity (ε) values were not immediately available however. Thus, the results were given for $\varepsilon = 4.5\%$ [23]. Fig. 5 compares the present empirical results with those given in the literature.

A high value for α of the aluminum ($\alpha = 97.1 \cdot 10^{-6}\mathrm{m^2/s}$ at 27℃ [23]) means a very effective heat diffusion over the plate surfaces. Those high experimental values observed in fig. 5 are due to the high α value of the aluminum making the plate temperatures approach to the ambient temperature of $T_\infty = 27.0775$℃ quite effectively. Air flow discontinuities were taken into consideration in the calculated h_{avg} values through temperature measurements. High α value of the aluminum causes the temperature measurements to be uncorrelated. This in turn makes the h_{avg} values uncorrelated. Although the temperature results of fig. 4 were calibrated, the measured temperature sensitivity of the results was apparent in fig. 5. The experimental results were not reliable on highly conductive surfaces.

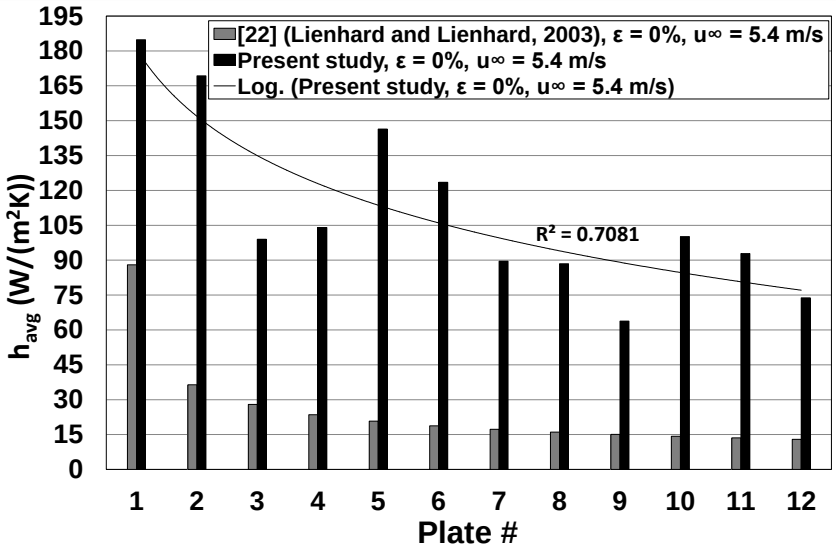

Fig. 5. Forced convective heat transfer coefficients on the horizontal flat plate. Literature and present empirical results compared. Present empirical results with $\varepsilon = 0\%$.

Extent of mass transfer was assessed: At a relative humidity of 30% and a room temperature of 27.0775℃, below about 7.8℃ chilling will be identified on the plate surfaces. Given a diffusivity coefficient of $2.6 \cdot 10^{-5}\mathrm{m}^2/\mathrm{s}$ at 1atm and 298K between water and air and $h_{avg} = 15.576\mathrm{W}/(\mathrm{m}^2\mathrm{K})$ (an average value for the natural convection heat transfer coefficient over the horizontal flat plate with $\varepsilon = 4.5\%$), the amount of the mass transfer from the wet plate surface into the air was calculated. These results were given in fig. 6.

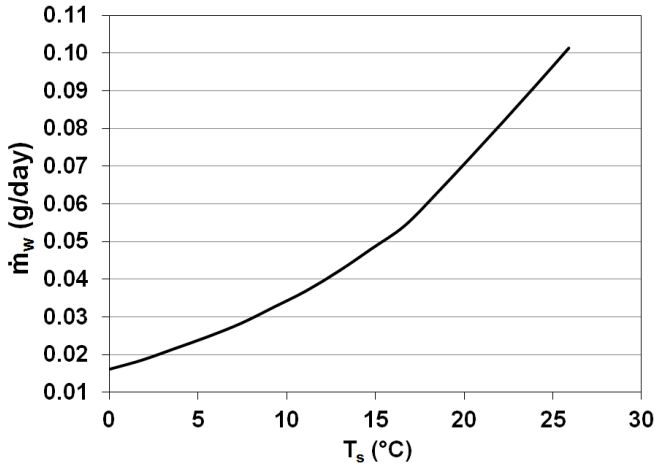

Fig. 6. The amount of mass transfer from the wet surface of a plate.

5.2. Horizontal flat plate: free convection

The plate temperatures as read out from the data loggers were shown in fig. 4. These temperature readings were calibrated against the twelve-plate average temperature. A correlation regarding the free convection coefficient on a horizontal flat plate is available in the literature [23]: $\overline{Nu}_{L_c} = 0.54Ra_{L_c}^{1/4}$, ($10^4 \lesssim Ra_{L_c} \lesssim 10^7$, $Pr \gtrsim 0.7$) where L_c is the characteristic length ($L_c = A/P$) with A (m^2) and P (m), respectively, representing the single-sided surface area and perimeter of the twelve plates. Ra (Rayleigh number) is defined as $Ra_{L_c} = Gr_{L_c}Pr = g\beta(T_s - T_\infty)L_c^3/(\nu\alpha)$ where g is the gravitational acceleration (m^2/s), β is the thermal expansion coefficient of air (K^{-1}), T_s is the surface temperature (K), T_∞ is the ambient air temperature (K), ν is the kinematic viscosity of air (m^2/s), and α is the thermal diffusivity of air (m^2/s). It was found that calculation of $\overline{Nu}_{L_c}$ with only one single plate having a surface area of $4 \cdot 10^{-4}\mathrm{m}^2$ produced a small Ra_{L_c} ($Ra_{L_c} = 127.0$) which was not able to reach the recommended correlation interval for Ra_{L_c}. Even with all the twelve plates put side-by-side ($A = 48 \cdot 10^{-4}\mathrm{m}^2$) it was found that $Ra_{L_c} \approx 3{,}693$, which still would not let the available $\overline{Nu}_{L_c}$ expression be used. It was calculated that a flat plate surface arrangement with a total surface area of at least ($A = 80 \cdot 10^{-4}\mathrm{m}^2$), that is, four rows of plates each with five plates, would be required for the $\overline{Nu}_{L_c}$ expression to be applicable ($Ra = 11{,}131$).

5.3. Vertical flat plate: free convection

A correlation regarding the free convection coefficients of the vertical flat plates is given [23]: $\overline{Nu}_L = 0.68 + 0.670Ra_L^{1/4}/[1 + (0.492/Pr)^{9/16}]^{4/9}$, $Ra_L \lesssim 10^9$. It is recommended [23] that in this $\overline{Nu}_L$ expression, $\Delta T_{L/2} = T_s(L/2) - T_\infty$ be used, that is, the temperature difference appearing in Ra_L expression is to be calculated at the midpoint of the flat plate geometry. In present arrangement, $L/2 = 0.12\mathrm{m}$ and $T_s(L/2)$

($\varepsilon = 0\%$) corresponded to the average of the empirical plate temperature measurements of the sixth and seventh plates, which was $T_s(L/2) = 62.0798$℃. Using this empirical value and applying a trial-and-error approach with $h_{avg} = q/(A\Delta T_{L/2})$, it was found $\Delta T_{L/2} = 79.3724$℃, $h_{avg} = 5.472\text{W}/(\text{m}^2\text{K})$, and $Ra_L = 5.777 \cdot 10^7$ for the literature values of the vertical flat plate. In other words, the literature values gave $T_s(L/2) = 106.45$℃ and $h_{avg} = 5.472\text{W}/(\text{m}^2\text{K})$) and the present empirical values gave ($T_s(L/2) = 62.0798$℃, $h_{avg} = 13.761\text{W}/(\text{m}^2\text{K})$). The literature and current empirical values presented absolute differences of about 44.370℃ ($T_s(L/2)$) and $7.966\text{W}/(\text{m}^2\text{K})$ ($T_s(L/2)$) for the vertical plate.

Because the present results were given experimentally for the constant surface temperatures of the plates, Nu change versus Ra was not possible with the surface temperature. This was the case for the natural convection over the horizontal or vertical flat plates.

5.4. Arbitrary-shape body: forced convection

Fig. 7 illustrates the arbitrary-shape body experimented. Plate numbers are as in the arrangement of fig. 2.

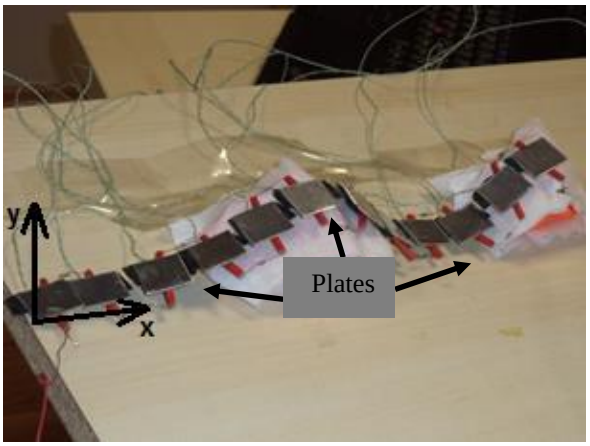

Fig. 7. Arbitrary-shape body created with twelve plates.

Table 1 lists the end point coordinates of the plates creating the arbitrary-shape body.

Table 1. Plate end point coordinates of the arbitrary-shape body.

plate #	1	2	3	4	5	6	7	8	9	10
x, cm	2.0	4.4	7.0	9.4	11.4	14.0	16.5	18.6	21.0	23.4
y, cm	0.6	0.8	1.2	2.4	3.0	3.4	2.4	0.9	0.4	1.3
plate #	11	12								
x, cm	24.8	26.9								
y, cm	3.3	4.3								

The empirical local convective heat transfer coefficients were included in fig. 8.

As the cooling intensified (that is, as $u_\infty = 4.0\text{m/s}$ increased to $u_\infty = 5.4\text{m/s}$), the plate temperatures leaned to approach the true ambient temperature ($T_\infty = 27.0775$℃) which rendered the calculated h_{avg} values large. Neglecting the radiation altogether ($\varepsilon = 0\%$) resulted in an increase on the h_{avg} values in fig. 8. Further increasing the radiation ($\varepsilon = 90\%$) resulted in a decrease on the h_{avg} values.

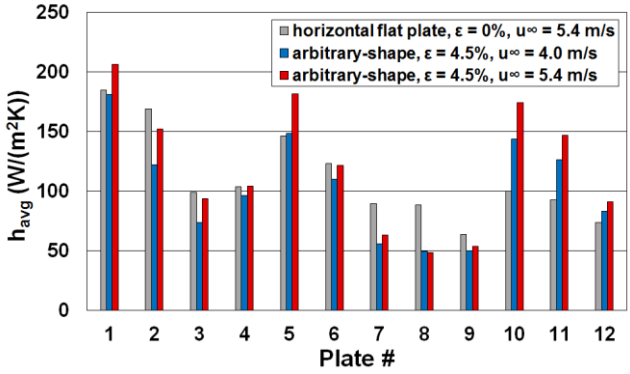

Fig. 8. Empirical (present) forced convection heat transfer coefficient (h_{avg}) values compared between the conductive horizontal flat plate results for $u_\infty = 5.4\text{m/s}$ ($\varepsilon = 0\%$) and the conductive arbitrary-shape body for $u_\infty = 4.0\text{m/s}$ ($\varepsilon = 4.5\%$) and $u_\infty = 5.4\text{m/s}$ ($\varepsilon = 4.5\%$).

6. Experimental Uncertainty

The accuracy of the empirical h_{avg} values was dependent on the accuracies of the plate and ambient temperature measurements: A differential in the form $df = \pm[\sum_{T=T_s,T_\infty}(\partial f/\partial T)^2(dT)^2]^{1/2}$ was given [24] where $f = h_{avg} = [q - \varepsilon A\sigma(T_s^4 - T_\infty^4)]/(A(T_s - T_\infty))$. The overall accuracy of the temperature measurements including the accuracies of the data logger ($dT_{dl} = \pm 0.2\%T \pm 0.5$℃) and that of the thermocouples ($dT_{th} = \pm 3.0\%T$, an estimate) was calculated from $dT = [(\pm 0.2\%T \pm 0.5\text{℃})^2 + (\pm 3.0\%T)^2]^{\frac{1}{2}}$. This procedure produced experimental uncertainties (dh_{avg}) that were larger than the size of the h_{avg} values. Figs. 9 and 10 show the empirical uncertainties based on the calculated h_{avg} values of fig. 8.

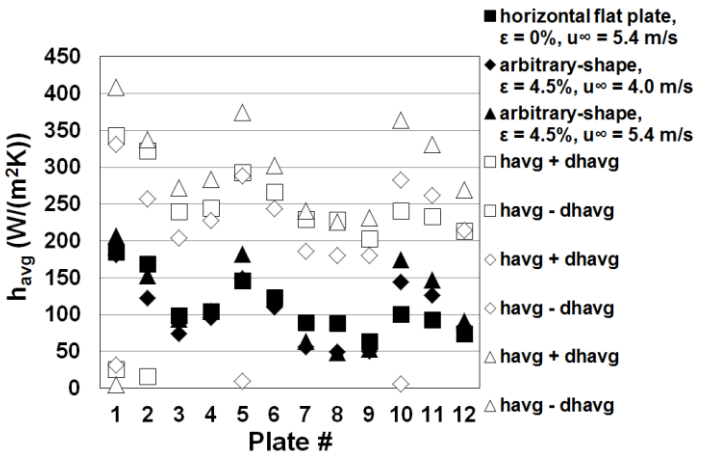

Fig. 9. Empirical uncertainty in the present case ($dT_{th} = \pm 3.0\%T$, $dT_{dl} = \pm 0.2\%T \pm 0.5$℃).

It was found that the reliability of the present experimental results was dependent on the individual accuracies of the thermocouple and the data loggers. Even a hundred times improvement on their accuracies ($dT_{dl} = \pm 0.002\%T \pm 0.5$℃) and ($dT_{th} = \pm 0.03\%T$) still resulted in comparatively large dh_{avg} values. This was depicted in fig. 10.

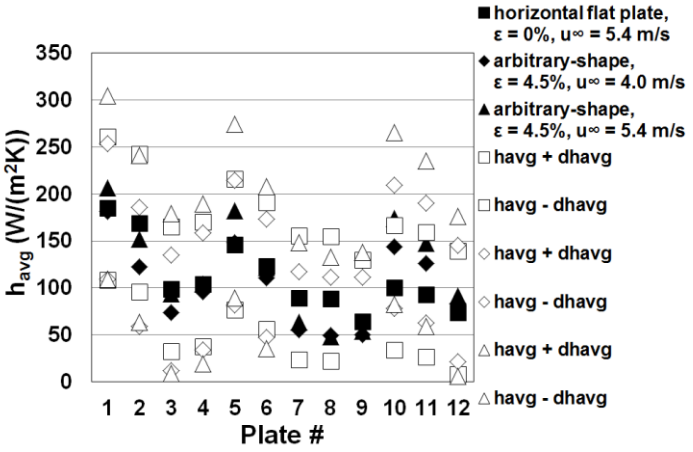

Fig. 10. Experimental uncertainty of the present case with the improved uncertainties ($dT_{th} = \pm 0.03\%T$, $dT_{dl} = \pm 0.002\%T \pm 0.5$℃).

Figs. 9 and 10 reflect the effect of plates' position on the convective heat transfer coefficients. Uncertainty is large signifying the measured temperature sensitivity of the convective heat transfer coefficients.

7. Conclusions

Experiments were performed to determine the local natural and local forced convective heat transfer coefficients over the flat and arbitrary-shape bodies. The flat surfaces and arbitrary-shape bodies were made of a highly conductive material. Local forced convective heat transfer coefficients were determined with the presence of air blowing over the plates. Air flow and buoyancy characteristics were incorporated in the present results via temperature measurements which meant the velocity and thermal boundary layer developments over the plates. After taking into account the irregular positioning of the thermocouples and electrical resistors at the plate surfaces, the acquired convective heat transfer coefficients were found to be uncorrelated. In this paper, an important point was identified which was the fact that aluminum material was an effective heat dissipater. As a result of this, cooling of the plates toward the vicinity of the ambient temperature gave large convective heat transfer coefficients. Thus, accurate convective heat transfer coefficients on the highly conductive structures were not possible experimentally.

Effective cooling was found possible with a conductive surface. A conductive surface with a high thermal diffusivity value was an effective cooler. The other highly conductive materials, for example, Cu, Ag, or Au might show same characteristics as a result of their high thermal diffusivity values. Natural or forced convective heat transfer coefficients on the non-conductive flat surfaces or arbitrary shapes were not intended here. Utilizing the current approach, an arbitrary-shape body with a high thermal diffusivity value can be tested; however, it is difficult to compare the natural or forced convective heat transfer coefficients in a realistic manner.

Nomenclature

Letter

A Surface area [m^2]

Bi Biot number [$= (h\Delta t)/k$]

g Gravitational acceleration [m/s^2]
Gr Grashof number [$= g\beta(T_s - T_\infty)L_c^3/\nu^2$]
h Convective heat transfer coefficient [$W/(m^2K)$]
I Current [A]
k Thermal conductivity [$W/(mK)$]
L Length [m]
Nu Nusselt number [$= (hx)/k$]
P Perimeter [m]
Pr Prandtl number [$= \nu/\alpha$]
q Power [W]
R Resistance [Ω]
Ra Rayleigh number [$= g\beta(T_s - T_\infty)L_c^3/(\nu\alpha)$]
Re Reynolds number [$= (u_\infty x)/\nu$]
T Temperature [K]
t Thickness [m]
u_∞ Air velocity [m/s]
x x-coordinate [m]
y y-coordinate [m]

Subscript

air Air
Al Aluminum
amb Ambient
avg Average
c Characteristic, central
dl Data logger
l Contact
p Plate
s Surface
th Thermocouple
1 Start point
2 End point
∞ Free stream

Greek

α Thermal diffusivity [m^2/s]
β Thermal expansion coefficient [K^{-1}]
Δ Finite [$-$]
ε Emissivity [%]
ν Kinematic viscosity [m^2/s]
σ Standard deviation [℃]

References

[1] Chen, C. -K. and Chen, C. -H., Nonuniform Porosity and Non-Darcian Effects on Conjugate Mixed Convection Heat Transfer from a Plate Fin in Porous Media, *International Journal of Heat and Fluid Flow, 11* (1990), 1, pp. 65-71

[2] Sun, C., Yu, B., Oztop, H. F., Wang, Y., and Wei, J., Control of Mixed Convection in Lid-Driven Enclosures Using Conductive Triangular Fins, *International Journal of Heat and Mass Transfer, 54* (2011), 4, pp. 894-909

[3] Hsiao, K. -L. and Hsu, C. -H., Conjugate Heat Transfer of Mixed Convection for Viscoelastic Fluid Past a Horizontal Flat-Plate Fin, *Applied Thermal Engineering, 29* (2009), 1, pp. 28-36

[4] Isaac, S. and Barnea, Y., Simple Analysis of Mixed Convection with Uniform Heat Flux, *International Journal of Heat and Mass Transfer, 29* (1986), 8, pp. 1139-1147

[5] Chen, T. S., Tien, H. C., and Armaly, B. F., Natural Convection on Horizontal, Inclined, and Vertical Plates with Variable Surface Temperature or Heat Flux, *International Journal of Heat and Mass Transfer, 29* (1986), 10, pp. 1465-1478

[6] Higuera, F. J. and Ryazantsev, Y. S., Natural Convection Flow Due to a Heat Source in a Vertical Channel, *International Journal of Heat and Mass Transfer, 45* (2002), 10, pp. 2207-2212

[7] Yian, L. Y., Amin, N., and Pop, I., Mixed Convection Flow Near a Non-orthogonal Stagnation Point Towards a Stretching Vertical Plate, *International Journal of Heat and Mass Transfer, 50* (2007), 23-24, pp. 4855-4863

[8] Shih, T. -M., Thamire, C., and Zhang, Y., Heat Convection Length for Boundary-layer Flows, *International Communications in Heat and Mass Transfer, 38* (2011), 4, pp. 405-409

[9] Hassani, A. V. and Hollands, K. G. T., Prandtl Number Effect on External Natural Convection Heat Transfer from Irregular Three-Dimensional Bodies, *International Journal of Heat and Mass Transfer, 32* (1989), 11, pp. 2075-2080

[10] Al-Sanea, S. A., Mixed Convection Heat Transfer Along a Continuously Moving Heated Vertical Plate with Suction or Injection, *International Journal of Heat and Mass Transfer, 47* (2004), 6-7, pp. 1445-1465

[11] Yang, Y. -T. and Wang, S. -J., Free Convection Heat Transfer of Non-Newtonian Fluids Over Axisymmetric and Two-dimensional Bodies of Arbitrary Shape Embedded in a Fluid-saturated Porous Medium, *International Journal of Heat and Mass Transfer, 39* (1996), 1, pp. 203-210

[12] Bianco, N. and Nardini, S., Numerical Analysis of Natural Convection in Air in a Vertical Convergent Channel with Uniformly Heated Conductive Walls, *International Communications in Heat and Mass Transfer, 32* (2005), 6, pp. 758-769

[13] Wilks, G., External Natural Convection About Two-dimensional Bodies with Constant Heat Flux, *International Journal of Heat and Mass Transfer, 15* (1972), 2, pp. 351-354

[14] Yovanovich, M. M., General Expression for Forced Convection Heat and Mass Transfer from Isopotential Spheroids, *Proceedings of the AIAA 26th Aerospace Sciences Meeting*, Reno, Nevada, 1998, AIAA 88-0743

[15] Hassani, A. V. and Hollands, K. G. T., A Simplified Method for Estimating Natural Convection Heat Transfer from Bodies of Arbitrary Shape, *Proceedings of the ASME 87-HT-11 National Heat Transfer Conference*, Pittsburg, Pennsylvania, USA, 1987

[16] Nakayama, A. and Shenoy, A., Turbulent Free Convection Heat Transfer to Power-law Fluids from Arbitrary Geometric Configurations, *International Journal of Heat and Fluid Flow, 12* (1991), 4, pp. 336-343

[17] Lee, S. L. and Lin, D. W., Transient Conjugate Heat Transfer on a Naturally Cooled Body of Arbitrary Shape, *International Journal of Heat and Mass Transfer, 40* (1997), 9, pp. 2133-2145

[18] Sepa Aluminum and Metal, http://www.sepa.com.tr

[19] Cem Instruments, http://www.cem-instruments.com

[20] Pico Technology, thermocouple, http://www.picotech.com/thermocouples.html

[21] Pico Technology, datalogger, http://www.picotech.com/thermocouple.html

[22] Lienhard IV, J. H. and Lienhard V, J. H., *A Heat Transfer Textbook*, third edition, Phlogiston Press, Massachusetts, USA, 2003, p. 309

[23] Bergman, T. L., Lavine, A. S., Incropera, F. P., and Dewitt, D. P., *Fundamentals of Heat and Mass Transfer,* seventh edition, John Wiley and Sons Inc., New Jersey, USA, 2011, pp. 446, 1008

[24] Taylor, J. R., *An Introduction to Error Analysis: The Study of Uncertainties in Physical Measurements*, second edition, University Science Books, California, USA, 1997, p. 75